Assessment of Pulse Arrival Time for Arterial Stiffness Monitoring on Body Composition Scales

Birutė Paliakaitė[a,*], Saulius Daukantas[a], Vaidotas Marozas[a,b]

[a] *Biomedical Engineering Institute, Kaunas University of Technology, K. Barsausko st. 59, LT-51423 Kaunas, Lithuania*
[b] *Department of Electronics Engineering, Kaunas University of Technology, Kaunas, Lithuania*

Abstract

This study presents a system that aims to estimate changes in arterial health status in an unobtrusive way. It might be especially useful in long-term self-monitoring of cardiovascular performance for the successful patients' treatment and empowerment. This system applies the electrocardiographic and impedance plethysmographic signals acquired using modified body composition scales for the calculation of pulse arrival time, which is directly related to arterial stiffness. The proposed device was tested in a cohort of 14 subjects. The modified scales were compared to the commercial PulsePen tonometer and the results showed significant relationship between these different devices ($r_s = 0.93$, $p < 0.01$). The system also showed the ability to track small pulse arrival time variations induced by paced respiration. These findings suggest that scales evaluating parameters of cardiovascular function have potential to become a convenient device for self-monitoring of arterial stiffness.

Keywords: unobtrusive long-term health monitoring, personal health technologies, multi-sensing device, impedance plethysmogram, slope sum function

1. Introduction

Elasticity and stiffness of large arteries have a considerable impact on cardiovascular (CV) function. These mechanical properties are responsible for maintaining continuous blood flow and retaining the shape of vessels under the high pressures. Therefore, changes in balance between elasticity and stiffness can contribute to the development of CV diseases, and target organ, such as heart, kidney and brain, damage [1–4].

It has been shown that an abnormal aortic stiffness is independently associated with an increased number of CV events, as well as to all-cause mortality [5, 6]. This especially applies to elderly population [7–9], patients with end-stage renal disease [10, 11], impaired glucose tolerance [12] and hypertension [3, 4, 13]. In addition, an increased aortic stiffness is found to be associated with microvascular brain lesions [14]. Although most of studies have been dedicated to the investigation of aortic arterial stiffness, the elastic properties of lower-limb arteries are also related to significant health issues, e.g., peripheral artery disease [15] and diabetic peripheral neuropathy [16].

Accordingly, periodic assessment of arterial stiffness has been suggested to be a part of long-term monitoring of target patients [2, 4, 5, 7–10, 12, 13]. Nevertheless, the technical concerns, notably, operator dependence and measurement standardization, restrict the inclusion of arterial stiffness characterizing parameters in clinical practice [17] and home-based monitoring. Therefore, a more convenient way for periodic estimation of arterial stiffness

*Corresponding author
Email addresses: birute.paliakaite@ktu.edu (Birutė Paliakaitė), saulius.daukantas@ktu.lt (Saulius Daukantas), vaidotas.marozas@ktu.lt (Vaidotas Marozas)

is highly desirable.

According to the Moens-Korteweg equation, elasticity of the arteries is inversely proportional to the time interval, required for the pulse wave to travel a fixed distance. A common approach is to assess the pulse arrival time (PAT) by employing the R-wave of the electrocardiogram (ECG) as a reference point and the pulse wave, recorded on a peripheral site (finger, toe). In this case, PAT is affected not only by the stiffness of the aortic arteries itself, but by the limb arteries as well. Therefore, this information can be valuable for evaluating general status of the arteries.

Emerging advances in technology enable integration of sensors for acquiring various physiological signals in an unobtrusive way. For example, bathroom scales with handlebar and footpad electrodes have been successfully applied to acquire ECG [18–22], impedance plethysmogram (IPG) [19–22], ballistocardiogram [18, 20–22] and lower-body electromyogram [20]. So far, commercial bathroom scales are capable of estimating total body composition and heart rate. Moreover, the integration of assessment of arterial stiffness would allow to track changes in arterial status and transform bathroom scales into multi-parametric device.

In this paper, we propose a system for estimation of PAT using body composition scales, modified to acquire ECG and IPG signals. The proposed system enables unobtrusive long-term monitoring of PAT changes over the time, therefore, may form a basis for periodic arterial stiffness assessment. This issue has already been addressed by our group in a preliminary study [23].

This paper is organised as follows. The proposed method is described in Section 2, followed by a description of the study population and the performance measures in Section 3. The results characterizing performance are presented in Section 4 and compared to a commercial device. The paper is finished with a discussion and conclusions (Section 5, Section 6).

2. Materials and methods

The principle of PAT estimation using body composition scales relies on synchronously recorded ECG and IPG signals. ECG was obtained using Einthoven extremity leads, whereas IPG was recorded from the soles placed on the footpad electrodes.

2.1. Physiological background

The morphology of IPG depends on local blood volume in the body [24]. IPG is obtained by stimulating tissue with low amplitude high frequency current. Since the amplitude of the current is constant, the voltage alternates according to the impedance changes occurring due to the changes in the blood volume. Given that the lower-body IPG signal is the sum of the local impedances of all the segments between the voltage measuring electrodes, the total impedance is affected by separate body parts differently. Hence, smaller cross sectional area and greater local impedance make the lower parts of the legs contribute more to the total impedance than the lower torso or thighs [25]. As a result, the IPG recorded on the bathroom scales mostly represents blood pulsation in the feet.

Generally, PAT depends on permanent arterial stiffness, but also varies with blood pressure in a short period of time because arteries become stiffer under increased pressure. Due to physiological phenomena, blood pressure and heart rate are already modulated at 0.1 Hz rate [26], yet paced breathing at the same rate additionally increases modulation. During inspiration effort the intrathoracic pressure falls and provokes the decrease in stroke volume. This causes the reduction of blood pressure and successive rise in PAT. At the same time, due to physiological effects heart rate increases to maintain cardiac output. During exhalation, the reverse is true [26]. Relationship between PAT and blood pressure is useful to evaluate the ability of the developed device to track small changes in PAT. These variations in hemodynamics are not instant but gradually

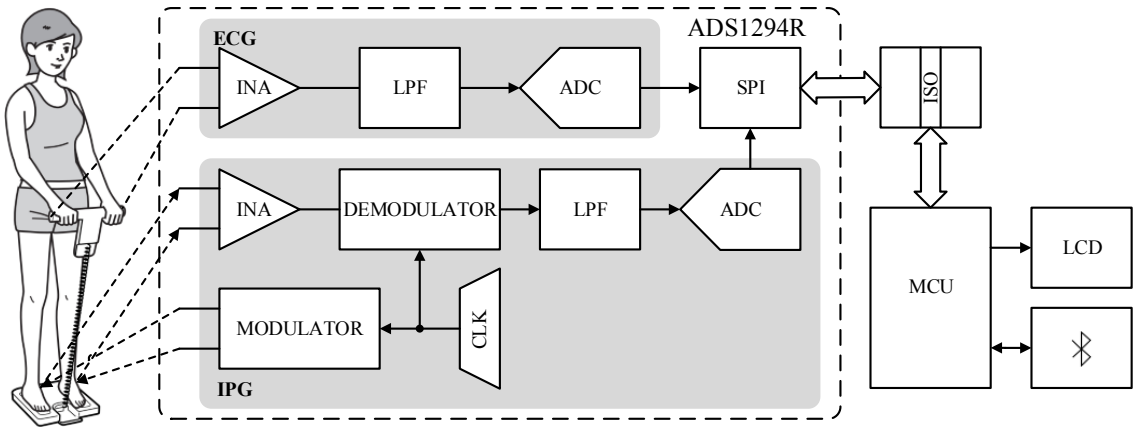

Fig. 1. Functional block diagram of instrumentation used for PAT estimation.

ongoing, so there is a time offset between changes in blood pressure, heart rate and PAT [27].

2.2. Instrumentation

Commercially available body composition scales with footpad and handlebar electrodes (HBF-510, Omron, Kyoto, Japan) were used in this study. The sensors of the scales were supplemented by the custom-made electronics for the purpose to acquire ECG and IPG. Functional block diagram of the measurement system is shown in Fig.1.

The analog front-end ADS1294R (Texas Instruments, Dallas, TX, USA) [28] was utilized for acquiring ECG and IPG. Two electrodes integrated in handlebar and one footpad electrode were used for obtaining 3 lead ECG, whereas two footpad electrodes below the heels were employed for recording the lower-body IPG. These footpad electrodes, connected to the integrated impedance measurement circuitry, were utilized to source 0.2 $\mathrm{mA_{rms}}$ constant harmonic current at 32 kHz into the body and to measure voltage drop. Signals were acquired synchronously at 500 Hz sampling rate.

2.3. Reference method

Recommended reference method for validation of non-invasive hemodynamic measurement devices is arterial tonometry [29]. It is usually performed on subjects in supine position, but the nature of our study requires them standing and operator leans his hand on subjects to achieve stability. If reference and proposed methods were performed synchronously, this contact would influence the results of the IPG recording mechanically and electrically. Thus, scales and tonometer are operated asynchronously in the present study.

Average PAT estimated using the proposed method was compared with calculated by the PulsePen (DiaTecne s.r.l., Milan, Italy) [30]. This device is composed of a tonometer and an integrated ECG unit. Pressure waves were recorded for at least 13 s simultaneously using tonometer placed on the posterior tibial artery of the right foot (see Fig. 2a). PAT_{R} was calculated as the time delay between the R-wave and the foot of the pressure wave using the included software. For the PulsePen the foot of the pressure wave is defined by the intersection of the horizontal line tangent to the lowest point of the pressure waveform with the extension of the line resulting from the mean square deviation of all points, building up the initial rise of the waveform [30]. Typical signals recorded with the PulsePen system are shown in Fig. 2b.

2.4. Signal processing

A block diagram of signal processing stages is presented in Fig. 3. ECG and IPG, defined as s_n and x_n, respectively, constitute the inputs of the algorithm (n is the index of the record sample). Only one lead out of 3 was

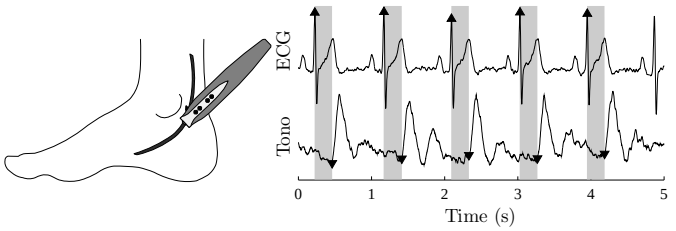

(a) (b)

Fig. 2. Reference method: (a) placement of the PulsePen on the posterior tibial artery; (b) example of the acquired signals. ▲ – R-wave, ▾ – foot of the pressure wave, grey area – estimated interval of PAT_{R}.

chosen depending on the quality of the ECG for each subject. The guiding rule when developing signal processing algorithm was to make it convenient for implementation on embedded system after slight modifications. Group delays of digital forward filters were taken into account and compensated for.

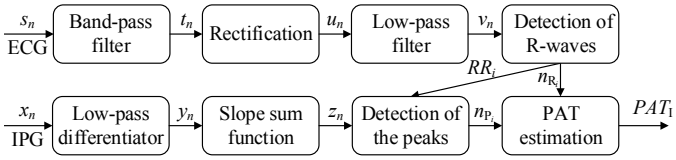

Fig. 3. Block diagram of signal processing stages.

The band-pass filtering of s_n was achieved by cascading recursive low-pass and high-pass filters. The pass-band from 12 to 18 Hz accentuates the QRS complexes, reduces the noise and the influence of the P and T waves. The transfer function of low-pass filter, described by cut-off frequency of 20 Hz and group delay of 7 samples, is given by

$$H_{lp}(z) = \frac{1}{64}\frac{(1-z^{-8})^2}{(1-z^{-1})^2}. \tag{1}$$

High-pass filter with cut-off frequency of 11.8 Hz and group delay of 16 samples was implemented by subtracting low-pass from all-pass filter. The transfer functions is defined by

$$H_{hp}(z) = z^{-16} - \frac{1}{32}\frac{(1-z^{-16})}{(1-z^{-1})}. \tag{2}$$

The output of the filters t_n was rectified in order to obtain positive peaks regardless of polarity of QRS complexes. After rectification the signal u_n was smoothed by low-pass filtering to eliminate unwanted peaks surrounding real R-waves. Recursive filter, characterized by cut-off frequency of 13.3 Hz and group delay of 11 samples, was used. The transfer function is defined by

$$H_{lp}(z) = \frac{1}{128}\frac{(1-z^{-12})^2}{(1-z^{-1})^2}. \tag{3}$$

The detection of the R-waves was performed by comparing the output of the low-pass filter v_n against the adaptive amplitude-dependent threshold. According to the timing of the R-waves $n_{\mathrm{R}i}$ (i is the index of the R-wave), the record was also divided into RR intervals. The length of each RR interval was determined as follows:

$$RR_i = n_{Ri} - n_{Ri-1}. \tag{4}$$

The signal x_n was processed with length 129 linear-phase low-pass-differentiator filter designed using least-squares error minimization method. This filter has the transition band from 9.4 to 14.4 Hz, the group delay of 64 samples and the edge frequency of 12 Hz. The output of the low-pass-differentiator y_n is the derivative of x_n with accentuated upslopes of the waveform, suppressed high-frequency noise and removed low-frequency drift.

The slope sum function was used to enhance the upslope even more and reduce the remainder of the waveform [31]. The output of this function z_n is defined as follows:

$$z_n = \sum_{k=n-w}^{n} h_k, \quad h_k = \begin{cases} y_k, & y_k > 0 \\ 0, & y_k \leqslant 0. \end{cases} \tag{5}$$

where w is the length of the analysing window. w was chosen empirically approximately equal to the duration of the upslope of the IPG waveform. In this study, w equals to 54 samples or 108 ms.

Peaks of the waveform were detected in z_n within each RR interval. $n_{\mathrm{P}i}$ is the timing of the ith peak. PAT for

every ith cardiac cycle PAT_{I} was estimated as the time difference between the time instant of the R-wave and the successive peak in the slope sum function:

$$PAT_{Ii} = n_{Pi} - n_{Ri}. \tag{6}$$

The output of the stages of signal processing and PAT_{I} estimation are presented in Fig. 4.

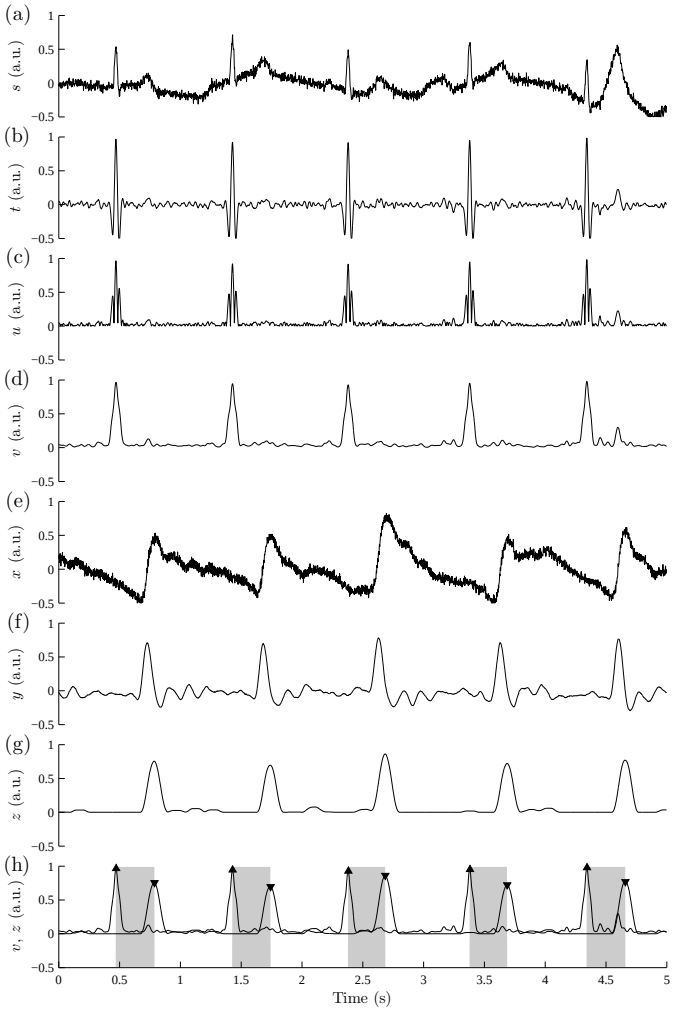

Fig. 4. Example of the stages of the ECG (from (a) to (d)) and IPG (from (e) to (g)) signals processing and PAT_{I} estimation (h). ▲ – n_{R}, ▼ – n_{P}, grey area – estimated interval of PAT_{I}.

3. Data collection and analysis

3.1. Subjects

Fourteen volunteer subjects (five female), from 22 to 81 years old, with body mass index (BMI) from 18.4 to 35.06 kg\m^2, were enrolled in the experiment. (see Table 1). Informed consent was obtained from all participants.

3.2. Measurement protocol

We measured PAT_{R} from the heart to the posterior tibial artery for every subject standing on the floor (Fig. 2a). Average PAT_{R} was obtained from the first ten heart cycles detected in the recording as suggested by the ARTERY Society [29]. Then, subjects were asked to stand still on the modified scales barefoot while holding handlebar electrodes in their lowered hands and breath normally. After waiting for the signals to stabilize, ECG an IPG were recorded for 1 min. In the end, subjects were instructed to synchronize their respiration with an on-screen bar graph indicator. Signals were registered for additional 1 min with deep paced (0.1 Hz) breathing.

3.3. Performance evaluation

Average PAT_{I} was also estimated from the first ten cardiac cycles of the bathroom scales recording. Average PAT_{I} and PAT_{R} (see Table 1) values for each subject were compared while analysing the recordings performed during normal breathing. Because of small data sample ($N = 14$), normal distribution of values could not be proven and non-parametric methods were chosen to evaluate the relationship and agreement between the methods. The statistical significance of observed difference between PAT_{R} and PAT_{I} was checked using Wilcoxon signed-rank test for paired samples. Additionally, correlation between subjects' age and PAT_{I} was investigated. In order to eliminate height influence on PAT_{I}, it was height-normalized (divided by subject's height).

For the repeatability and reliability evaluation of the proposed method the first 50 cardiac cycles of each subject during normal breathing were used. Estimated PAT_{I} values were divided into five segments and corresponding average PAT_{I} was calculated for each segment. Thus, five

Table 1. Data for the subjects in this study.

Subject information					Normal breathing		Paced breathing	
No.	**Sex**	**Age (y)**	**Height (cm)**	**BMI (kg\m^2)**	**PAT$_R$ (ms)**	**PAT$_I$ (ms)**	**Lag (beats)**	**r$_{max}$**
1	F	45	172	18.9	218.0	293.6	0.75	0.73
2	M	81	172	24.0	191.4	256.4	4.00	0.27
3	M	33	186	22.8	246.4	326.8	3.75	0.79
4	M	28	181	23.5	242.2	317.2	5.00	0.85
5	F	27	168	22.3	229.8	276.2	4.00	0.67
6	M	31	179	22.8	230.2	302.0	4.50	0.71
7	M	22	172	23.7	250.0	327.2	3.75	0.51
8	M	26	187	21.4	267.2	326.8	5.75	0.75
9	M	23	185	35.1	263.6	332.8	10.75	0.33
10	M	24	185	26.3	273.6	342.4	4.25	0.82
11	F	23	165	22.0	283.4	361.0	6.50	0.53
12	M	45	182	26.3	222.7	292.2	3.50	0.67
13	F	22	176	18.4	286.8	327.8	4.00	0.74
14	F	76	169	24.2	207.6	273.2	5.00	0.45

average PAT_{I} values per subject made up 70 values in total. Intraclass correlation (ICC) and coefficient of repeatability (CR) with their confidence intervals were calculated according to [32]. ICC is a measure of reliability relating the magnitude of the measurement error in observed measurements to the characteristic variability in underlying values between subjects. CR is the greatest absolute difference expected between the two measurements on the same subject under the identical conditions in the future.

To examine the effectiveness of multi-parametric scales in detection of small changes in PAT, we evaluated the relationship between RR and PAT_{I} for each subject during paced breathing in 1 min length record. Firstly, each vector of calculated RR and PAT_{I} values was processed with 3-points median filter to eliminate the outliers. Then, additional values of RR and PAT_{I} were estimated by linear interpolation at each quarter of the beat. Finally, normalized product-moment cross-correlation functions r of RR against PAT_{I} were calculated. The lag in RR changes outrunning PAT_{I} changes, where correlation function reaches its maximum amplitude $r_{\max}$, was located for each subject (Table 1).

4. Results

4.1. Estimated PAT values

Examples of the typical ECG and IPG signals during normal breathing in 1 min and 10 s length intervals are shown in Fig. 5. Baseline wandering (see Fig. 5a) is mainly caused by respiration, but motion and changes in electrode impedance (dry metal electrodes were used in the study) also have an influence on it. Moreover, high frequency noise from EMG is present and ambient noise can be induced in case of poor electrode-skin contact as well. Nevertheless, the quality of the signals is sufficient for detection of the R-waves and the upslopes of the pulse waveform.

Different effects of normal and deep paced breathing on PAT_{I} and RR variability are illustrated in Fig. 6. Fig. 6b displays a typical pattern of RR and PAT_{I} variations with time driven at the respiratory period of 10 s. It is evident that RR changes outrun PAT_{I} changes.

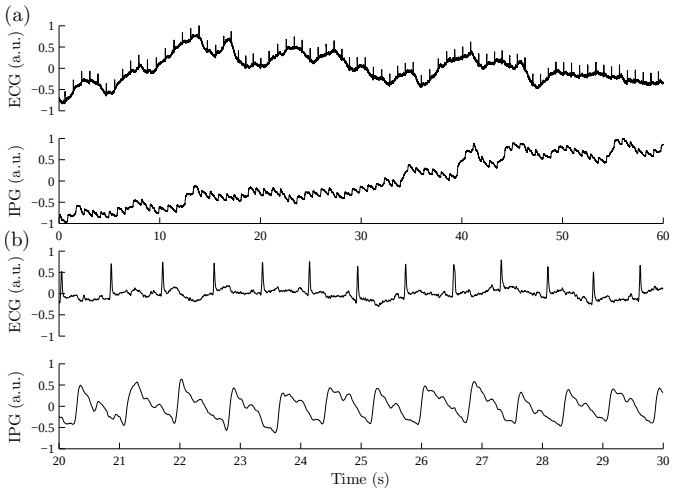

Fig. 5. Examples of the ECG and IPG signals acquired by developed multi-parametric scales: (a) unprocessed 1 min length record and (b) 10 s interval of band-pass filtered signals (0.5 to 40 Hz).

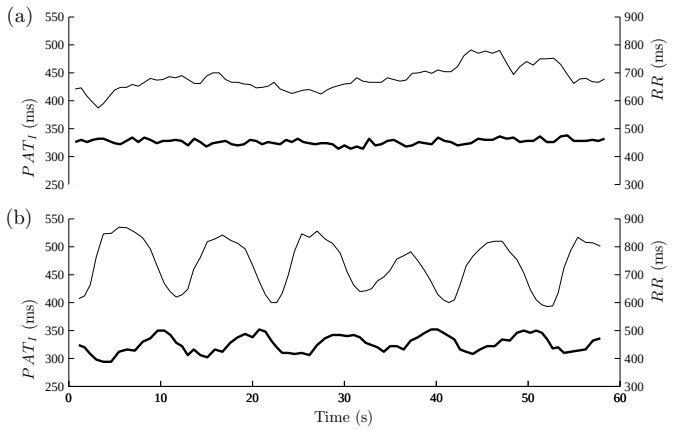

Fig. 6. PAT_{I} (thick lines) and RR (thin lines) changes during (a) normal and (b) paced breathing (subject No.13).

4.2. Comparison with the reference method

PAT_{I} values are prolonged with respect to PAT_{R} values and the median difference is -69.35 ms (95% CI=-75.3 to -62.3 ms) (see Fig. 7a). Average PAT values estimated with different devices agree well as the 80% limits of agreement are from -77.88 to -45.86 ms (10th and 90th percentiles). Scatter plot in Fig. 7b displays relationship between PAT_{I} and PAT_{R}. Spearman's rank correlation coefficient between these two variables $r_s = 0.93$ ($p < 0.01$).

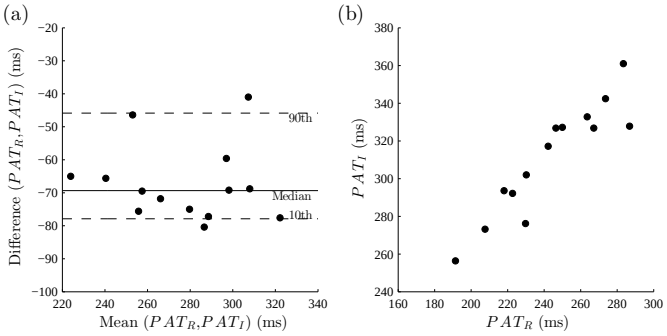

Fig. 7. Agreement and relationship between PAT values estimated with modified body composition scales and PulsePen tonometer: (a) the Bland-Altman plot and (b) the scatter plot.

4.3. Correlation with age

Calculated Spearmans's rank correlation coefficient as an estimate of correlation between subjects' age and height-normalized PAT_{I} was $r_s = -0.87$ ($p < 0.01$). It corresponds to the statement that the decrease in PAT is related to ageing.

4.4. Reliability and repeatability

The calculated estimate of reliability was ICC=0.988 (95% CI=0.975 to 0.996), where between- and within-subject standard deviations were 30.11 ms and 3.31 ms, respectively. ICC shows that measurement errors are small in comparison to the true differences between subjects. The coefficient of repeatability for this study is relatively small CR=9.16 ms (95% CI=7.73 ms to 11.24 ms).

4.5. Evaluation of induced PAT variation

The maximum amplitude of changes in RR ranged from 67 to 222 ms and in PAT_{I} from 30 to 76 ms across all subjects during paced respiration. The correlation functions of the oldest subject (No.2) and the subject with the highest BMI (No.9) showed poor results reaching the maximum amplitude of 0.27 and 0.33 only (Table 1), therefore, were excluded from the further study. The maximum amplitudes of correlation function ranged from 0.45 to 0.85 with RR changes outrunning the PAT_{I} changes from 0.75 to 6.5 beats for other individual subjects. The mean correlation function of these subjects reached a maximum

amplitude of $r = 0.58$ with the lag of 4.23 ± 1.41 beats (mean±SD). Individual and mean cross-correlation functions for subjects with RR and PAT_{I} relationship are displayed in Fig. 8.

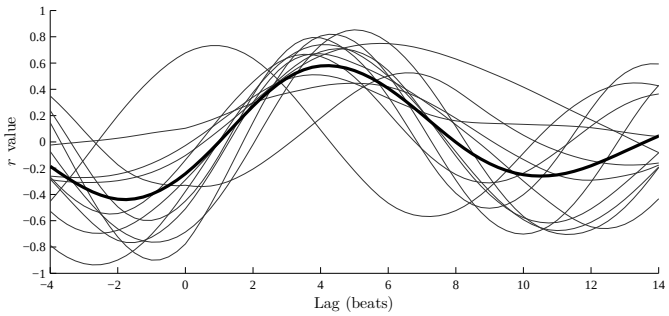

Fig. 8. Cross-correlation functions of RR against PAT_{I} for all subjects with respiratory sinus arrhythmia and baroreflex (thin lines). Thick line indicates the mean of all cross-correlation functions displayed.

5. Discussion

5.1. Principal findings

As mentioned in [33], the novel personal health technologies are likely to be successful only if they clearly reduce inconveniences and burden for patients, helping them to accomplish their "work" more efficiently and effectively. The proposed system takes a step towards meeting these requirements. The present study was carried out in order to evaluate the ability of the modified scales to assess PAT and track its changes. Results of the experiment showed that unobtrusive multi-sensing device in a form of simple bathroom scales with integrated IPG and ECG electrodes is capable of acquiring signals suitable for cardiovascular parameters estimation. It should be noted that the proposed device is intended to monitor changes in arterial health status rather than calculate absolute estimates of arterial stiffness.

In comparison with previous work [23], the custom-made electronics instead of commercial data acquisition system was used in this research. We were free to choose frequency and amplitude of the excitation current for the IPG measurement; hence, desirable quality of the signals and low noise level were achieved. Also, digital signal processing algorithm was improved.

In the first part of the study we compared average PAT values estimated with multi-parametric scales to the PulsePen findings. The results indicated significant relationship between the two methods ($r_s = 0.93$, $p < 0.01$). Also, the limits of agreement were no wider than 32 ms but the PulsePen device produced 70 ms smaller values of PAT. This distinction could be explained by different PAT definitions and body places used for signal acquisition. The PulsePen uses the foot of the pulse wave as the fiducial point, whereas our method - maximum of the slope sum function, which corresponds approximately to the maximum of the first derivative. These particularities of the processing methods contributed to the difference between PAT_{R} and PAT_{I} values the most. Additionally, electrodes for the IPG acquisition were in contact with subject's heels, while tonometer was placed higher, on the posterior tibial artery. Distance between these locations added up to the different estimation of PAT.

Every procedure with the PulsePen tonometer requires an experienced operator, but the measurement is still hard to perform while subject is standing. Because of anatomical differences between participants of the experiment, difficulties arose when palpating posterior tibial artery for some of them and the measurement outlasted usual procedure. On the contrary, the IPG signal was present and easily recorded for all the subjects standing on the body composition scales. Furthermore, the use of this device is straightforward and the final version is supposed to be completely operator-independent. Dry electrodes on the scales are far more practical than disposable ones used by the PulsePen as well. In comparison with the PulsePen, which position can vary between subjects, operators and measurements, the scales have an advantage as the electrodes are placed exactly under the heels.

As could be predicted, strong relationship was found

between subjects' age and height-normalized PAT_{I} values estimated with body composition scales ($r_s = -0,87$, $p < 0.01$). The obtained correlation is in line with common knowledge, based on longitudinal studies [7–9], that arterial stiffness increases with ageing. The results imply that the proposed device is capable of assessing this ageing phenomenon.

In this study, the estimated reliability was high (ICC=0.988). Hence, we draw the conclusion that variability in measurements is due to genuine differences in PAT_{I} between subjects rather than to errors in the measurement process. Therefore, subjects can be well distinguished in terms of PAT. However, estimated ICC depends upon variability in PAT between subjects measured (standard deviation was 30.11 ms), so it is only true in the population of similar heterogeneity. Performed repeatability analysis also brought a decent coefficient. It suggests that any two measurements made on a particular subject with constant underlying PAT value are estimated to differ by no more than 9.16 ms on 95 % of occasions. This time interval can be ascribed only to errors due to the measurement process itself.

The second part of the study was designed to assess the suitability of the proposed system for the estimation of small changes in PAT. These changes were induced by paced breathing and evaluated against simultaneous variations in RR intervals. Although relationship between heart rate and PAT variabilities is indirect and lagged, some individual cross-correlation functions of RR against PAT_{I} reached maximum amplitude of $r = 0.7$ and more. Consequently, we suppose that the proposed device is capable of tracking variation in PAT. The mean time of lag between RR and PAT_{I} was 4 beats but for individual subjects it varied from 1 to 7 beats. Moreover, maximum variability in length of RR intervals and PAT was different across the subjects. Therefore, further research is needed to understand the physiological importance and application of parameters defining cardiorespiratory relations.

We investigated beat-to-beat changes of PAT in this study and the bathroom scales were able to distinguish between them. It is possible to apply this property for the evaluation of the respiratory sinus arrhythmia or baroreflex sensitivity. However, beat-to-beat tracking of PAT is less valuable in long-term monitoring, which helps to track changes in arterial stiffness after various pharmacological (antihypertensive treatment, treatments of congestive heart failure, hypolipidaemic, antidiabetic agents, AGE-breakers) or non-pharmacological (exercise training, dietary changes, hormone replacement therapy) interventions [1]. Unfortunately, there is no generally accepted practice on optimal timing and frequency of cardiovascular health assessment in healthy or low-risk persons but it is likely to be a part of standard patient follow-up in high cardiovascular risk persons [17]. Nevertheless, it has been shown that time to change of arterial stiffness is relatively fast (weeks or months) [3]; consequently, we suspect day-to-day or week-to-week changes in PAT may be more practical to follow.

5.2. Comparison with prior work

Studies carried out in [18–22] employed modified bathroom scales too. Some of them were focused on signal-to-noise ratio improvement, EMG usage for the detection of motion artefacts or fusion of the signals to develop robust systems for CV monitoring at home [20, 21]. However, studies in [20, 21] have not provided any specific CV parameter. Experiments in [18] were dedicated to determine changes in subject's cardiac output and contractility using ECG and BCG signals. The rest of the studies were focused on heart rate detection from IPG or BCG, or both signals [19, 22]. None of the mentioned investigations were interested in PAT estimation and arterial stiffness assessment.

The work by Gomez-Clapers et al. [34] is the closest in nature to the present study. The suitability of the IPG for the estimation of PAT with a handheld device was in-

vestigated. The method showed valid agreement with that based on photoplethysmography. Nevertheless, the upper-body IPG was used in [34] and its practical healthcare application was not specified.

Relationship between RR intervals and PAT during paced respiration was examined in [27]. The mean cross-correlation function reached the maximum amplitude of $r = 0.69$ with the lag of 3.17 beats. The experiments were carried out on the subjects in supine position using ECG and finger photoplethysmographic signals. This is an advantage since respiratory related changes of heart rate are larger in supine than standing position [26] and motion artefacts are negligible. The present study did not include the additional minute before recording to allow subject's respiratory depth to stabilize. Still, our findings are consistent with that in [27].

5.3. Limitations

Blood pressure changes were induced through paced respiration. However, periodic variations in RR and PAT_{I} were missing in some cases. The outlier can be explained by disorder or absence of respiratory sinus arrhythmia or baroreflex sensitivity. Thus, another method for inducing PAT changes is preferable. Exercising is frequently used because it raises blood pressure. Nevertheless, this method would be more challenging to implement as continuous measurement would be prevented and should be taken in stages. Another solution is longitudinal study but it is time-consuming.

As previously mentioned, IPG recorded between the feet is determined mostly by the lower parts of the legs. The location of the electrodes is always ascertained but the true source of the IPG signal is not. While high frequency current is used, moisture of the skin has a negligible impact on its conductivity [25]. On the other hand, the resistivity of the tissues depends on temperature, water content and blood perfusion [25]. Furthermore, IPG represents blood volume, which resistivity is also temperature, hematocrit and flow dependent [35]. Changes in all these factors may be pathologically induced or arise from shift in environmental parameters (e.g. cold room). Alterations in the shape of the waveform due to electrical properties of the tissues may affect the results of timing. Thus, additional analysis may provide information on the repeatability of the IPG signal source and its reproducibility under the influence of various physiological effects.

5.4. Future directions

The methodology of the study slightly differs from that recommended in ARTERY Society guidelines [29]. It concerns devices that assess pulse wave velocity but can also be adapted to PAT estimating devices in a thoughtful way. Firstly, larger population of subjects with reasonable gender and age balance should be included. The study would be enriched if the experiments were prolonged to several hours or days and a number of recordings were present for each subject, which would allow more credible reliability and repeatability estimation. Measurements in the present experiments were performed during a short period of time while standing and breathing normally, so blood pressure was unlikely to change, accordingly, its values were not presented. However, blood pressure would be valuable in explaining any large variations in measurement during extended study.

Sampling rate used in our experiments is 500 Hz but the one suggested by ARTERY Society is 1 kHz [29]. This limitation is partially overcome by PAT_{I} averaging. However, amplification of sampling rate is considered. Note that the PulsePen used in this study also has a sampling rate of 500 Hz, hence, a device with higher sampling rate should be considered as a reference method for more accurate comparison.

The experiments of this paper were performed in laboratory environment and adequate quality of the signals was achieved. However, adaptation of the multi-parametric scales for long-term periodic monitoring of CV function

in unsupervised environment remains a great challenge. Considerable amount of effort should be put in improvement of the noise immunity and quality of the signals. The strain gauges from the scales and EMG signals could be employed to increase reliability of the system by cancelling signals corrupted with artefacts. Incorporation of additional health parameters also would broaden the field of application of the proposed device.

6. Conclusions

This paper shows that the proposed scales can estimate pulse arrival time, which may be used for arterial stiffness evaluation. The present system has potential to be applied for unobtrusive long-term self-monitoring of cardiovascular patients. Furthermore, these scales could be extended to a multi-parametric device by supplementing with additional parameters thus becoming an attractive way for tracing health status of general population.

Conflict of interest statement

None to declare.

Acknowledgment

This work was partly supported by the projects "Promotion of Student Scientific Activities" (VP1-3.1-ŠMM-01-V-02-003) from the Research Council of Lithuania and CARRE (No. 611140), funded by the European Commission Framework Programme 7. Also, the authors would like to thank Dr. A. Petrėnas for his valuable comments and suggestions on the manuscript.

References

[1] S. Laurent, J. Cockcroft, L. Van Bortel, P. Boutouyrie, C. Giannattasio, D. Hayoz, B. Pannier, C. Vlachopoulos, I. Wilkinson, H. Struijker-Boudier, Expert consensus document on arterial stiffness: methodological issues and clinical applications, Eur. Heart J. 27 (21) (2006) 2588–2605. doi:10.1093/eurheartj/ehl254.

[2] C. Vlachopoulos, K. Aznaouridis, C. Stefanadis, Prediction of cardiovascular events and all-cause mortality with arterial stiffness: a systematic review and meta-analysis, J. Am. Coll. Cardiol. 55 (13) (2010) 1318–1327. doi:10.1016/j.jacc.2009.10.061.

[3] G. Mancia, R. Fagard, K. Narkiewicz, J. Redon, A. Zanchetti, M. Bohm, T. Christiaens, R. Cifkova, G. D. Backer, A. Dominiczak, M. Galderisi, D. E. Grobbee, T. Jaarsma, P. Kirchhof, S. E. Kjeldsen, S. Laurent, A. J. Manolis, P. M. Nilsson, L. M. Ruilope, R. E. Schmieder, P. A. Sirnes, P. Sleight, M. Viigimaa, B. Waeber, F. Zannad, 2013 ESH/ESC Guidelines for the management of arterial hypertension, Blood Press. 22 (4) (2013) 193–278. doi:10.3109/08037051.2013.812549.

[4] G. F. Mitchell, Arterial stiffness and hypertension, Hypertension 64 (1) (2014) 13–18. doi:10.1161/HYPERTENSIONAHA.114.00921.

[5] T. Willum Hansen, J. A. Staessen, C. Torp-Pedersen, S. Rasmussen, L. Thijs, H. Ibsen, J. Jeppesen, Prognostic value of aortic pulse wave velocity as index of arterial stiffness in the general population, Circulation 113 (5) (2006) 664–670. doi:10.1161/CIRCULATIONAHA.105.579342.

[6] G. F. Mitchell, S. Hwang, R. S. Vasan, M. G. Larson, M. J. Pencina, N. M. Hamburg, J. A. Vita, D. Levy, E. J. Benjamin, Arterial stiffness and cardiovascular events: the Framingham Heart Study, Circulation 121 (4) (2010) 505–511. doi:10.1161/CIRCULATIONAHA.109.886655.

[7] S. Meaume, A. Benetos, O. Henry, A. Rudnichi, M. Safar, Aortic pulse wave velocity predicts cardiovascular mortality in subjects >70 years of age, Arterioscler. Thromb. Vasc. Biol. 21 (12) (2001) 2046–2050. doi:10.1161/hq1201.100226.

[8] K. Sutton-Tyrrell, S. S. Najjar, R. M. Boudreau, L. Venkitachalam, V. Kupelian, E. M. Simonsick, R. Havlik, E. G. Lakatta, H. Spurgeon, S. Kritchevsky, M. Pahor, D. Bauer, A. Newman, Health ABC Study, Elevated aortic pulse wave velocity, a marker of arterial stiffness, predicts cardiovascular events in well-functioning older adults, Circulation 111 (25) (2005) 3384–3390. doi:10.1161/CIRCULATIONAHA.104.483628.

[9] F. U. Mattace-Raso, T. J. van der Cammen, A. Hofman, N. M. van Popele, M. L. Bos, M. A. Schalekamp, R. Asmar, R. S. Reneman, A. P. Hoeks, M. M. Breteler, J. C. Witteman, Arterial stiffness and risk of coronary heart disease and stroke: the Rotterdam Study, Circulation 113 (5) (2006) 657–663. doi:10.1161/CIRCULATIONAHA.105.555235.

[10] J. Blacher, A. P. Guerin, B. Pannier, S. J. Marchais, M. E. Safar, G. M. London, Impact of aortic stiffness on survival in end-stage renal disease, Circulation 99 (18) (1999) 2434–2439. doi:10.1161/01.CIR.99.18.2434.

[11] T. Shoji, M. Emoto, K. Shinohara, R. Kakiya, Y. Tsujimoto,

H. Kishimoto, E. Ishimura, T. Tabata, Y. Nishizawa, Diabetes mellitus, aortic stiffness, and cardiovascular mortality in end-stage renal disease, J. Am. Soc. Nephrol. 12 (10) (2001) 2117–2124.
URL http://jasn.asnjournals.org/content/12/10/2117.abstract

[12] K. Cruickshank, L. Riste, S. G. Anderson, J. S. Wright, G. Dunn, R. G. Gosling, Aortic pulse-wave velocity and its relationship to mortality in diabetes and glucose intolerance: an integrated index of vascular function?, Circulation 106 (16) (2002) 2085–2090. doi:10.1161/01.CIR.0000033824.02722.F7.

[13] S. Laurent, P. Boutouyrie, R. Asmar, I. Gautier, B. Laloux, L. Guize, P. Ducimetiere, A. Benetos, Aortic stiffness is an independent predictor of all-cause and cardiovascular mortality in hypertensive patients, Hypertension 37 (5) (2001) 1236–1241. doi:10.1161/01.HYP.37.5.1236.

[14] G. F. Mitchell, M. A. van Buchem, S. Sigurdsson, J. D. Gotal, M. K. Jonsdottir, Ó. Kjartansson, M. Garcia, T. Aspelund, T. B. Harris, V. Gudnason, L. J. Launer, Arterial stiffness, pressure and flow pulsatility and brain structure and function: the Age, Gene/Environment Susceptibility – Reykjavik Study, Brain 134 (11) (2011) 3398–3407. doi:10.1093/brain/awr253.

[15] H. Yokoyama, T. Shoji, E. Kimoto, K. Shinohara, S. Tanaka, H. Koyama, M. Emoto, Y. Nishizawa, Pulse wave velocity in lower-limb arteries among diabetic patients with peripheral arterial disease, J. Atheroscler. Thromb. 10 (4) (2003) 253–258. doi:10.5551/jat.10.253.

[16] M. Edmonds, V. Roberts, P. Watkins, Blood flow in the diabetic neuropathic foot, Diabetologia 22 (1) (1982) 9–15. doi:10.1007/BF00253862.

[17] P. Greenland, J. S. Alpert, G. A. Beller, E. J. Benjamin, M. J. Budoff, Z. A. Fayad, E. Foster, M. A. Hlatky, J. M. Hodgson, F. G. Kushner, M. S. Lauer, L. J. Shaw, S. C. Smith, Jr, A. J. Taylor, W. S. Weintraub, N. K. Wenger, 2010 ACCF/AHA Guideline for assessment of cardiovascular risk in asymptomatic adults, J. Am. Coll. Cardiol. 56 (25) (2010) e50–e103. doi:10.1016/j.jacc.2010.09.001.

[18] O. Inan, M. Etemadi, A. Paloma, L. Giovangrandi, G. Kovacs, Non-invasive cardiac output trending during exercise recovery on a bathroom-scale-based ballistocardiograph, Physiological Measurement 30 (3) (2009) 261. doi:10.1088/0967-3334/30/3/003.

[19] D. Díaz, O. Casas, R. Pallas-Areny, Heart rate detection from single-foot plantar bioimpedance measurements in a weighing scale, in: Engineering in Medicine and Biology Society (EMBC), 2010 Annual International Conference of the IEEE, 2010, pp. 6489–6492. doi:10.1109/IEMBS.2010.5627358.

[20] O. Inan, D. Park, L. Giovangrandi, G. Kovacs, Noninvasive measurement of physiological signals on a modified home bathroom scale, IEEE Trans. Biomed. Eng. 59 (8) (2012) 2137–2143. doi:10.1109/TBME.2012.2186809.

[21] J. Gomez-Clapers, R. Casanella, R. Pallas-Areny, Multi-signal bathroom scale to assess long-term trends in cardiovascular parameters, in: Engineering in Medicine and Biology Society (EMBC), 2012 Annual International Conference of the IEEE, 2012, pp. 550–553. doi:10.1109/EMBC.2012.6345990.

[22] D. Park, O. Inan, L. Giovangrandi, A combined heartbeat detector based on individual BCG and IPG heartbeat detectors, in: Engineering in Medicine and Biology Society (EMBC), 2012 Annual International Conference of the IEEE, 2012, pp. 3428–3431. doi:10.1109/EMBC.2012.6346702.

[23] B. Paliakaite, S. Daukantas, A. Sakalauskas, V. Marozas, Estimation of pulse arrival time using impedance plethysmogram from body composition scales, in: Sensors Applications Symposium (SAS), 2015 IEEE, 2015, pp. 1–4. doi:10.1109/SAS.2015.7133577.

[24] J. Malmivuo, R. Plonsey, Bioelectromagnetism: principles and applications of bioelectric and biomagnetic fields, Oxford University Press, New York, 1995.

[25] S. Grimnes, O. G. Martinsen, Bioimpedance and Bioelectricity Basics, 3rd Edition, Elsevier (Academic Press), London, 2014.

[26] E. Kaniusas, Biomedical Signals and Sensors I, 1st Edition, Springer-Verlag Berlin Heidelberg, 2012. doi:10.1007/978-3-642-24843-6.

[27] M. J. Drinnan, J. Allen, A. Murray, Relation between heart rate and pulse transit time during paced respiration, Physiol. Meas. 22 (3) (2001) 425. doi:10.1088/0967-3334/22/3/301.

[28] Low-power, 8-channel, 24-bit analog front-end for biopotential measurements, Tech. Rep. ADS1294R, Texas Instruments, Dallas, TX, USA, Rev. J (January 2014).
URL http://www.ti.com/lit/ds/symlink/ads1294r.pdf

[29] I. B. Wilkinson, C. M. McEniery, G. Schillaci, P. Boutouyrie, P. Segers, A. Donald, P. J. Chowienczyk, ARTERY society guidelines for validation of non-invasive haemodynamic measurement devices: Part 1, arterial pulse wave velocity, Artery Research 4 (2) (2010) 34 – 40. doi:http://dx.doi.org/10.1016/j.artres.2010.03.001.

[30] P. Salvi, G. Lio, C. Labat, E. Ricci, B. Pannier, A. Benetos, Validation of a new non-invasive portable tonometer for determining arterial pressure wave and pulse wave velocity: the PulsePen device, J. Hypertens. 22 (12) (2004) 2285 – 2293.
URL http://journals.lww.com/jhypertension/Fulltext/2004/12000/Validation_of_a_new_non_invasive_portable.10.aspx

[31] W. Zong, T. Heldt, G. Moody, R. Mark, An open-source algorithm to detect onset of arterial blood pressure pulses, in:

Computers in Cardiology, 2003, Vol. 30, 2003, pp. 259–262. doi:10.1109/CIC.2003.1291140.

[32] J. W. Bartlett, C. Frost, Reliability, repeatability and reproducibility: Analysis of measurement errors in continuous variables, Ultrasound Obstet. Gynecol. 31 (4) (2008) 466–475. doi:10.1002/uog.5256.

[33] J. S. Ancker, H. O. Witteman, B. Hafeez, T. Provencher, M. Van de Graaf, E. Wei, "You Get Reminded You're a Sick Person": Personal data tracking and patients with multiple chronic conditions, J. Med. Internet Res. 17 (8) (2015) e202. doi:10.2196/jmir.4209.

[34] J. Gomez-Clapers, R. Casanella, R. Pallas-Areny, Pulse arrival time estimation from the impedance plethysmogram obtained with a handheld device, in: Engineering in Medicine and Biology Society, EMBC, 2011 Annual International Conference of the IEEE, 2011, pp. 516–519. doi:10.1109/IEMBS.2011.6090093.

[35] L. A. Geddes, L. E. Baker, The specific resistance of biological material—a compendium of data for the biomedical engineer and physiologist, Med. Biol. Eng. 5 (3) (1967) 271–293. doi:10.1007/BF02474537.